Dyes and Pigments 82 (2009) 353–359

Contents lists available at ScienceDirect

Dyes and Pigments

journal homepage: www.elsevier.com/locate/dyepig

Novel fluoranthene dyes for efficient dye-sensitized solar cells

Xuemei Ma [a], Wenjun Wu [a], Qiong Zhang [a,b], Fuling Guo [a], Fanshun Meng [a], Jianli Hua [a,*]

[a] Key Laboratory for Advanced Materials and Institute of Fine Chemicals, East China University of Science and Technology, Shanghai 200237, PR China
[b] Theoretical Chemistry, School of Biotechnology, Royal Institute of Technology, S-10691 Stockholm, Sweden

ARTICLE INFO

Article history:
Received 29 December 2008
Received in revised form
9 February 2009
Accepted 11 February 2009
Available online 25 February 2009

Keywords:
Dye-sensitized solar cells
Fluoranthene
Synthesis
Characterization
Nanocrystalline TiO_2
Photovoltaic properties

ABSTRACT

Three, novel, fluoranthene-based dyes, 2-cyano-3-(5-(7,12-diphenylbenzo[*k*]fluoranthen-3-yl)thiophen-2-yl)acrylic acid, 2-(5-((5-(7,12-diphenylben-zo[*k*]fluoranthen-3-yl)thiophen-2-yl)methylene)-4-oxo-2-thioxothiazolidin-3-yl)acetic acid and 2-cyano-3-(4-(2-(7,12-diphenylbenzo[*k*]fluoranthen-3-yl)ethynyl) phenyl) acrylic acid, were synthesized for application as sensitizers in dye-sensitized solar cells. In each dye, the 7,12-diphenyl-benzo[*k*]fluoranthene moiety acted as electron donor with phenyl and thiophene units as electron spacers and carboxylic acid as electron acceptor. Tuning of the HOMO and LUMO energy levels was conveniently accomplished by changing the spacer and acceptor moiety, as confirmed using electrochemical measurements. Maximum solar energy:electricity conversion efficiency was 4.4% under AM 1.5 solar simulator (100 mW cm^{-2}) for 2-cyano-3-(5-(7,12-diphenylbenzo[*k*]fluoranthen-3-yl) thiophen-2-yl)acrylic acid. The results suggest that dyes based on fluoranthene donor are promising candidates for high performance, dye-sensitized solar cells.

1. Introduction

Dye-sensitized solar cells (DSSCs) have attracted great attention because of their relatively higher efficiency and low cost compared with conventional inorganic devices. Up to now, DSSCs based on the Ru-complex dyes can produce photoelectric conversion yield of 11% under standard AM 1.5 sun light irradiation, which is sufficiently high to be of practical utility [1,2]. However, the large-scale application of ruthenium dyes is limited because of costs and environmental issues. So more and more efforts have been dedicated to the development of pure organic dyes which exhibit not only higher molar extinction coefficients, but also simple preparation and purification procedure at lower cost [3]. Recently, several groups have developed pure organic sensitizers to overcome the prohibitive issues of ruthenium metal complexes, and the impressive photovoltaic performance has been obtained with some organic coumarin [4], indoline [5], oligoene [6], hemicyanine [7], and cyanine dyes [8] having efficiencies in the range of 5–9%. These results indicated that pure organic dyes would be a promising type of sensitizers for dye-sensitized solar cells and it is necessary to develop novel pure organic sensitizers.

Fluoranthene is a polycyclic aromatic hydrocarbon (PAH) with intense fluorescence, which has been applied to electrogenerated chemiluminescence (ECL), such as in display devices, in the analytical determination of PAHs in minute concentrations, and as labels in immunoassay [9]. Due to the extended π-electron systems in such molecules, charge carriers in molecules can be excited by light in the visible spectral range and this fact increases their potential applicability as dye-sensitizers for DSSCs. However, to the best of our knowledge, chromophores containing fluoranthene structural motifs have not been exploited for DSSCs. Based on the above consideration, we have designed and synthesized three novel organic sensitizers **F1**, **F2** and **F3** (shown in Fig. 1), which consist of 7,12-diphenylbenzo[*k*] fluoranthene moiety acting as electron donor, phenyl and thiophene units as electron spacers and carboxylic acid as electron acceptor. The carboxylic acid group is introduced as an anchoring group toward nanocrystalline TiO_2. Meanwhile, three novel sensitizers have been applied successfully to sensitization of nanocrystalline TiO_2-based solar cells and the corresponding photovoltaic properties, electronic and optical properties are presented in this paper.

2. Experimental

2.1. General procedure

^1H NMR and ^{13}C NMR spectra were recorded on a spectrometer operating at 400 and 100 MHz. MS were recorded on EI or ESI mass spectroscopy. UV–vis spectra were determined with a Varain Cary 500 spectrometer. Fluorescent spectra were recorded on Varian

* Corresponding author. Tel.: +86 21 64250940; fax: +86 21 64252758.
E-mail address: jlhua@ecust.edu.cn (J. Hua).

0143-7208/$ – see front matter © 2009 Elsevier Ltd. All rights reserved.
doi:10.1016/j.dyepig.2009.02.006

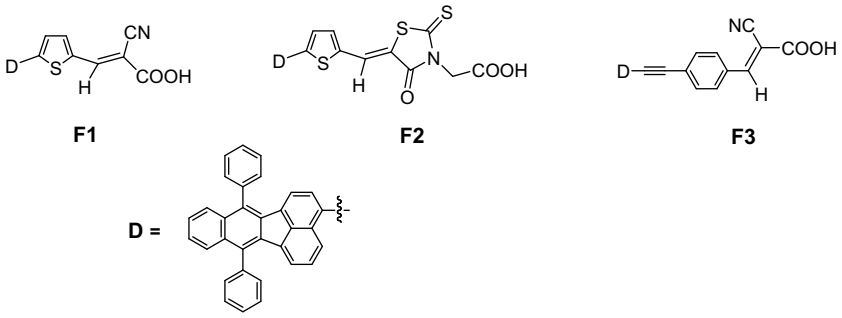

Fig. 1. Molecular structures of dyes (**F1**–**F3**).

Cary Eclipse Fluorescence spectrophotometer. The cyclic voltammograms of dyes were estimated with a Versastat II electrochemical workstation using a normal three-electrode cell with a Pt working electrode, a Pt wire auxiliary electrode, and Ag/AgCl reference electrode in saturated KCl solution. Tetrabutylammonium hexaflourophosphate (TBAPF6) 0.1 M was used as the supporting electrolyte in CH_2Cl_2.

2.2. Materials

Optically transparent FTO conducting glass (fluorine doped SnO_2, transmission >90% in the visible, sheet resistance 15 Ω/square) was obtained from the Geao Science and Educational Co. Ltd. of China and cleaned by a standard procedure. Titanium (IV) isopropoxide and 3-methyl-2-oxazolidinone were purchased from Aldrich. Lithium iodide was from Fluka. All other solvents and chemicals used were produced by Sinopharm Chemical Reagent Co., Ltd., China (reagent grade) and used as received. Starting materials 1,3-diphenylisobenzofuran (**1**) and 5-bromoacenaphthylene (**2**) were synthesized and purified according to the established procedure [10]. Solvents were distilled from appropriate reagents.

2.3. Preparation of dye-sensitized nanocrystalline electrode TiO_2

The preparation of dye-sensitized TiO_2 electrode was prepared by following the procedure reported in the literature. TiO_2 colloidal dispersion was made according to Ref. [11] which employed commercial TiO_2 (P25, Degussa AG, Germany) as material. Films of nanocrystalline TiO_2 colloidal on FTO were prepared by sliding a glass rod over the conductive side of the FTO. Sintering was carried out at 450 °C for 30 min. Before immersion in the solution of dyes, these films were soaked in the 0.2 M aqueous $TiCl_4$ solution overnight in a closed chamber, which has been proved to increase the short-circuit photocurrent significantly. The thickness of the TiO_2 film was about 6 μm. After being washed with deionized water and fully rinsed with ethanol, the films were heated again at 450 °C followed by cooling to 80 °C and dipping into a 3×10^{-4} M solution of dye in methanol for 12 h at room temperature. The dye-coated TiO_2 film, as working electrode, was placed on top of an ITO glass as a counter electrode, on which Pt was sputtered. The redox electrolyte was introduced into the interelectrode space by capillarity force.

2.4. Photoelectrochemical measurements

The photoelectrochemical experiments were performed in sandwich-type two electrode cells. The dye-coated film was used as working electrode, platinized FTO glass as counter electrode and 0.5 M LiI + 0.05 M I_2 in acetonitrile and 3-methyl-2-oxazolidinone (volume ratio: 9:1) mixture solution as electrolyte. The photocurrent action spectra were measured with a Model SR830 DSP Lock-In Amplifier and a Model SR540 Optical Chopper (Stanford Research Corporation, USA), a 7IL/PX150 xenon lamp and power supply, and a 7ISW301 Spectrometer. The irradiation source for the photocurrent density–voltage (J–V) measurement is an AM 1.5 solar simulator (91160, Newport Co., USA). The incident light intensity was 100 mW cm^{-2} calibrated with a standard Si solar cell. The tested solar cells were masked to a working area of 0.15 cm^2. Volt–current characteristics were performed on Model 2400 Sourcemeter (Keithley Instruments, Inc., USA).

2.5. Synthesis

2.5.1. 3-Bromo-7,12-diphenylbenzo[k]fluoranthene (**3**) [12]

Compound **1** (6.88 g, 25.48 mmol) and **2** (4.25 g, 18.40 mmol) were refluxed in xylene (60 mL) for 24 h. After cooling to room temperature, petroleum (290 mL) ether was added and the precipitate was then filtered and used in the next step without further purification. The precipitate and trifluoroacetic acid (5.75 mL) were refluxed in dichloromethane (60 mL) for 18 h. After cooling to room temperature, the precipitate was then filtered and further washed using dichloromethane and given pure **3** as a yellow powder (yield 50.6%). ^{1}H NMR ($CDCl_3$, 500 MHz), δ: 7.88 (d, J = 8.0 Hz, 1H), 7.61–7.72 (m, 8H), 7.51–7.58 (m, 5H), 7.37–7.44 (m, 3H), 6.62 (d, J = 6.8 Hz, 1H), 6.40 (d, J = 7.6 Hz, 1H).

2.5.2. 5-(7,12-Diphenylbenzo[k]fluoranthen-3-yl) thiophene-2-carbaldehyde (**4**)

A stirred mixture of **3** (0.24 g, 0.50 mmol), 5-formylthiophen-2-ylboronic acid (0.078 g, 0.50 mmol), $Pd(PPh_3)_4$ (0.0075 g, 0.0065 mmol), Na_2CO_3 (1.00 g, 9.4 mmol), THF(10 mL) and H_2O (2 mL) was heated at reflux for 24 h. When the reaction was completed, water was added to quench the reaction. The product was extracted with dichloromethane. The organic layer was collected, dried over anhydrous $MgSO_4$. The precipitate was purified by column chromatography on silica (CH_2Cl_2/petrol ether = 1:1 v/v) to yield **4** as an orange solid (yield 90.0%). ^{1}H NMR (DMSO-d_6, 500 MHz), δ: 9.96 (s, 1H), 8.12 (s, 1H), 8.09 (d, J = 8.4 Hz, 1H), 7.74 (m, 6H), 7.67 (d, J = 7.5 Hz, 1H), 7.61 (d, J = 3.9 Hz, 1H), 7.53 (m, 9H), 6.57 (t, J = 6.98 Hz, 2H). ^{13}C NMR ($CDCl_3$, 125 MHz), δ: 183.3, 152.3, 144.0, 139.1, 139.1, 138.6, 137.7, 137.3, 136.5, 136.1, 135.8, 135.2, 134.4, 133.7, 133.5, 130.7, 130.5, 130.3, 130.2, 130.1, 129.9, 129.7, 129.6, 128.8, 128.7, 128.3, 128.2, 128.1, 127.5, 127.4, 126.9, 126.8, 126.6, 124.3, 123.3, 122.3. HRMS (m/z) [M] calcd for $C_{37}H_{22}OS$: 514.1391 found: 514.1390.

2.5.3. 4-(2-(7,12-Diphenylbenzo[k]fluoranthen-3-yl)ethynyl)benzaldehyde (**5**)

Compound **3** (0.40 g, 0.83 mmol), 4-ethynylbenzaldehyde (0.11 g, 0.83 mmol), PPh_3 (2.9 mg, 0.01 mmol), $Pd(PPh_3)_2Cl_2$ (2.9 mg, 0.01 mmol) and CuI (5.2 mg, 0.02 mmol) were added in

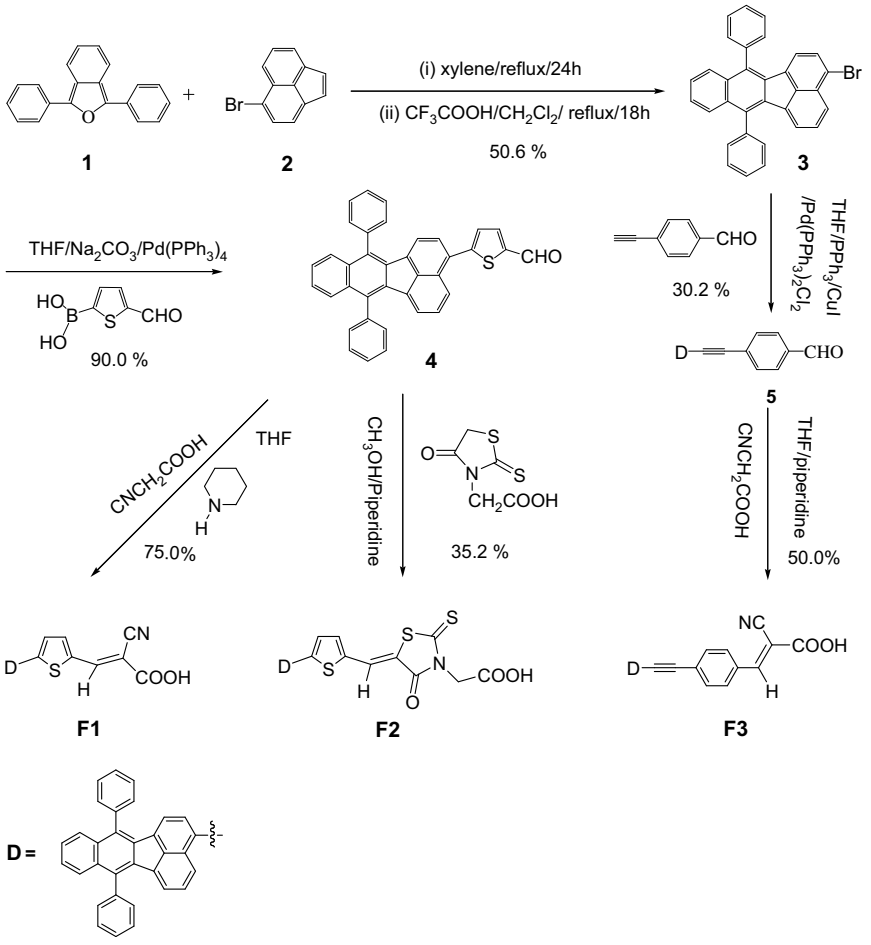

Scheme 1. Synthetic route of dyes (**F1**–**F3**).

20 mL triethylamine. The mixture was stirred in Ar atmosphere under reflux for 12 h. After the solvent was removed by rotate evaporator, the residue was extracted with chloroform and water. The organic layer was collected, dried over anhydrous $MgSO_4$. The precipitate was purified by column chromatography on silica (CH_2Cl_2/petrol ether = 1:2 v/v) to yield **5** as a yellow solid (yield 30.2%). ^{1}H NMR ($CDCl_3$, 500 MHz), δ: 10.04 (s, 1H), 8.07 (d, J = 8.0 Hz, 1H), 7.90 (m, 2H), 7.76 (m, 2H), 7.62–7.73 (m, 8H), 7.55–7.59 (m, 5H), 7.39–7.45 (m, 3H), 6.64 (d, J = 6.8 Hz, 1H), 6.58 (d, J = 7.2 Hz, 1H). ^{13}C NMR ($CDCl_3$, 125 MHz), δ: 192.0, 139.3, 139.2, 138.5, 137.7, 136.3, 136.1, 136.0, 135.9, 135.3, 134.7, 133.9, 133.8, 133.6, 133.3, 133.0, 132.9, 132.8, 130.6, 132.2, 132.2, 131.0, 130.9, 130.6, 130.3, 129.9, 129.4, 129.2, 129.1, 128.8, 128.7, 127.6, 127.5, 126.8, 126.7, 124.9, 123.5, 122.3, 119.3, 94.6, 92.3. HRMS (m/z) [M] calcd for $C_{41}H_{24}O$: 532.1827 found: 532.1831.

2.5.4. 2-Cyano-3-(5-(7,12-diphenylbenzo[k]fluoranthen-3-yl)thiophen-2-yl) acrylic acid (*F1*)

Compound **4** (0.13 g, 0.25 mmol), cyanoacetic acid (0.085 g, 1 mmol) and piperdine (0.5 mL) were added in 15 mL THF. The mixture was stirred in Ar atmosphere under reflux for 4 h. After cooling the solution, the organic layer was removed by rotate evaporator. The precipitate was purified by column chromatography on silica (CH_2Cl_2/ethanol = 1:1 v/v) to yield **F1** as an orange solid. (yield 75.0%).^{1}H NMR (DMSO-d_6, 500 MHz), δ: 8.23 (s, 1H), 8.08 (d, J = 8.4 Hz, 1H), 7.84 (s, 1H), 7.72 (m, 6H), 7.62 (d, J = 7.5 Hz, 1H), 7.56 (m, 10H), 6.56 (m, 2H); ^{13}C NMR (DMSO-d_6, 125 Hz), δ: 165.8, 148.6, 144.2, 140.7, 139.8, 139.8, 139.8, 139.4, 138.9, 138.7, 138.3, 137.9, 137.2, 137.0, 136.9, 135.8, 135.1, 134.5, 134.4, 132.0, 131.9, 131.6, 131.2, 130.8, 130.5, 130.4, 130.2, 129.2, 128.6, 128.6, 128.5, 128.5, 128.3, 128.0, 125.9, 124.9, 124.2, 123.7, 120.4, 108.9. HRMS (m/z) [M] calcd for $C_{40}H_{23}NO_2S$: 582.1528, found: 582.1507.

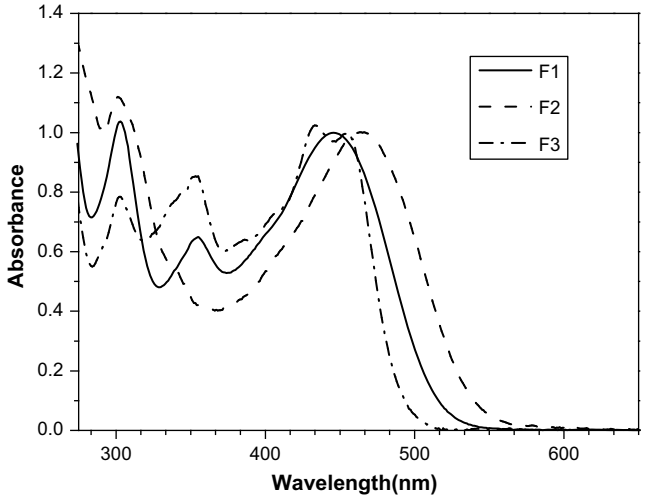

Fig. 2. Normalized absorption spectra of dyes in CH_2Cl_2.

Table 1
Optical and electrochemical properties of F1, F2 and F3.

Dye	λ_{max}[a] (nm) ($\varepsilon \times 10^{-4}$ M^{-1} cm^{-1})	λ_{max}[b] (nm)	λ_{em}[c] (nm)	Dye load[d] (mmol cm^{-3})	HOMO (eV) [e]	LUMO (eV) [e]
F1	445 (2.7), 354 (1.8), 302 (2.8)	440	589	114	−5.10	−2.80
F2	464 (1.5), 339 (0.8), 301 (1.6)	479	589	64	−5.06	−2.87
F3	433 (1.9), 352 (1.6), 302 (1.5)	432	589	131	−5.24	−2.83

[a] Absorption maximum in CH_2Cl_2.
[b] Absorption maximum on TiO_2 film.
[c] Emission maximum of dyes in CH_2Cl_2, **F1**, **F2** and **F3** are excited at 445, 464 and 433 nm, respectively.
[d] The dye loads are calculated from absorbance data of the sensitized TiO_2 electrodes.[20]
[e] HOMO is derived by a comparison with the ionization potential of ferrocene, scan rate, 100 mV s^{-1}; LUMO is calculated from the oxidation potential and the energy at the absorption threshold wavelength of dyes.

2.5.5. 2-(5-((5-(7,12-Diphenylbenzo[k]fluoranthen-3-yl)thiophen-2-yl)methylene)-4-oxo-2-thioxothiazolidin-3-yl)acetic acid (*F2*)

Compound **4** (0.10 g, 0.19 mmol), rhodanic acid (0.075 g, 0.38 mmol), piperidine (0.5 mL) were added in 10 mL methanol. The mixture was stirred in Ar atmosphere under reflux for 4 h. After cooling the solution, the organic layer was removed by rotate evaporator. The precipitate was purified by column chromatography on silica (CH_2Cl_2/ethanol = 1:1 v/v) to yield **F2** as a red solid (yield 35.2%) ^{1}H NMR (DMSO-d_6, 500 Hz), δ: 8.13 (s, 1H), 8.05 (d, J = 8.4 Hz, 1H), 7.73 (d, J = 4.2 Hz, 1H), 7.66 (s, 6H), 7.48 (m, 10H), 7.35 (m, 2H), 6.47 (d, J = 7.5 Hz, 1H), 4.67 (s, 2H); ^{13}C NMR (DMSO-d_6, 125 Hz), δ: 191.8, 174.5, 167.2, 148.9, 137.7, 137.6, 136.2, 135.1, 134.8, 133.7, 133.0, 132.4, 132.3, 129.7, 129.5, 129.4, 129.3, 129.2, 129.0, 128.9, 128.6, 128.4, 128.0, 127.9, 127.6, 127.5, 127.4, 126.9, 126.8, 126.5, 126.4, 125.9, 125.4, 124.3, 124.3, 123.9, 123.4, 123.4, 122.9, 121.5, 119.1, 45.1. HRMS (m/z) [M] calcd for $C_{42}H_{25}NO_3S_3$: 688.1075, found: 688.1074.

2.5.6. 2-Cyano-3-(4-(2-(7,12-diphenylbenzo[k]fluoranthen-3-yl)ethynyl)phenyl)acrylic acid (*F3*)

The synthesis method resembles compound **F1**, and the compound was purified by column chromatography on silica (CH_2Cl_2/ethanol = 1:2 v/v) to yield **F3** as a yellow solid (yield: 50.0%). ^{1}H NMR (DMSO-d_6, 500 Hz), δ: 8.31 (s, 1H), 8.11 (d, J = 8.4 Hz, 1H), 7.95 (m, 4H), 7.73 (m, 8H), 7.55 (m, 8H), 6.53 (t, J = 7.6 Hz, 2H); ^{13}C NMR (DMSO-d_6, 125 Hz), δ: 163.0, 146.9, 137.6, 137.5, 136.7, 136.1, 135.4, 134.9, 134.4, 133.7, 133.3, 133.0, 132.5, 132.3, 132.2, 132.0, 131.9, 131.8, 130.9, 129.8, 129.6, 129.6, 129.5, 129.4, 129.4, 129.2, 128.9, 128.7, 128.4, 128.3, 128.0, 126.6, 126.5, 126.4, 126.4, 124.3, 124.2, 122.4, 121.3, 118.6, 118.4, 113.3, 94.9, 89.3, 78.5. HRMS (m/z) [M] calcd for $C_{44}H_{25}NO_2$: 600.1963, found: 600.1959.

3. Results and discussion

3.1. Synthesis

The brief synthetic route of three organic dyes containing fluoranthene is depicted in Scheme 1. The synthesis of the dyes was carried out under classical procedures. Compound **3** was synthesized and purified according to the established procedure [12]. The important intermediates 5-(7,12-diphenylbenzo[k] fluoranthen-3-yl)thiophene-2-carbaldehyde (**4**) and 4-(2-(7,12-diphenylbenzo[k] fluoranthen-3-yl)ethynyl)benzaldehyde (**5**) were prepared from **3** by Suzuki [13] or Sonogashira [8] coupling reaction, respectively. The target products (**F1**–**F3**) were synthesized via Knoevenagel condensation reaction of the respective carbaldehydes with cyanoacetic acid or rhodanine-3-acetic acid in the presence of piperidine. All the intermediates and target dyes (**F1**–**F3**) were characterized by standard spectroscopic methods.

3.2. Absorption properties in solutions and on TiO_2 film

Absorption spectra of all compounds in dilute solution of CH_2Cl_2 are shown in Fig. 2 and the data are listed in Table 1. **F1** and **F3** have very similar absorption properties. **F1** and **F3** display two visible bands, appearing at 354/445 nm (18 000/27 000 M^{-1} cm^{-1}) and 352/433 nm (16 000/19 000 M^{-1} cm^{-1}), respectively, which are due to the π–π^* electron transition of the conjugated molecule; see TDDFT calculations below. Compared to **F3**, the absorption band of **F1**, bearing a thiophene moiety instead of a phenyl ring, presented slight red-shift absorption and higher maximum extinction coefficients (ε_{max}), manifesting the effect of thiophene unit in increasing conjugation and the molar extinction coefficient. For **F2**, one of the corresponding absorptions is red-shifted to 464 nm (15 000 M^{-1} cm^{-1}), which interprets that the rhodanine-3-acetic acid extends the π-conjugation system of dye through the 4-oxo-2-thioxothiazolidine ring [14], the other one is blue-shifted to 339 nm appearing as a shoulder peak. All these three chromophores show a strong band in the UV region at about 302 nm. The absorption bands of 301–354 nm are ascribed to the localized aromatic π–π^* electron transition and the absorption bands 433–464 nm are of intramolecular charge-transfer character. The absorption spectra of the dyes (**F1**–**F3**) on TiO_2 film are shown in Fig. 3. The absorption spectra of dyes attached to TiO_2 film are all broadened significantly compared with those in CH_2Cl_2 solution, implying that the dye aggregates are formed on the TiO_2 surface. The broadened absorption of all dyes loaded on the TiO_2 film is advantageous for light harvesting of the solar spectrum. The absorption peaks of the dyes **F1** and **F3** on TiO_2 film have slightly blue-shifted band

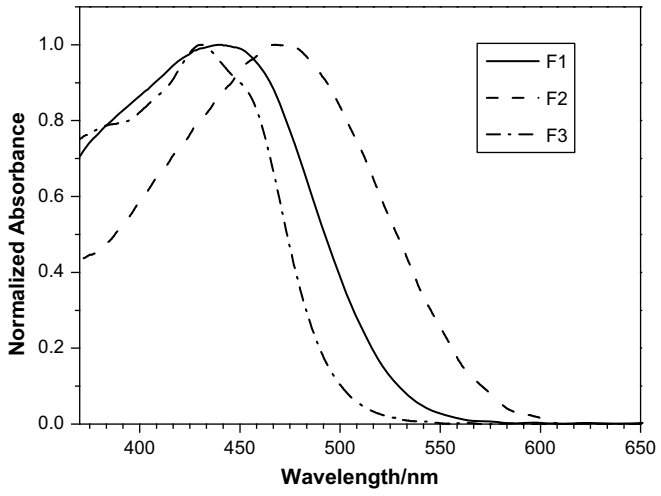

Fig. 3. Absorption spectra of dyes recorded in the TiO_2 film.

compared to those of the corresponding solution spectra, which is probably due to the H-aggregation. By contrast, the absorption peak of dye **F2** on TiO_2 film has a red-shifted band, which is probably due to the J-aggregation [8,15].

3.3. Electrochemical properties

For the photo-induced electron injection into TiO_2, it is necessary that the energy level of the excited state of the dye is higher than that of conduction band of TiO_2. To judge the possibility of electron transfer from the excited dye to the conduction band of TiO_2, the differential pulse voltammograms (DPVs) of the three dyes were measured in CH_2Cl_2 solution, using Ag/AgCl as a reference electrode, 0.1 M tetrabutylammonium hexafluorophosphate as a supporting electrolyte. The examined highest occupied molecular orbital (HOMO) levels and the lowest unoccupied molecular orbital (LUMO) levels are listed in Table 1. HOMO levels of −5.10 eV for **F1**, −5.06 eV for **F2** and −5.24 eV for **F3** were measured. With reference to the absorption maxima of 539 nm (2.30 eV), 567 nm (2.19 eV), 514 nm (2.41 eV), corresponding to the gap between the HOMO and LUMO levels for **F1**, **F2** and **F3**, respectively, the energy levels of the LUMO can be estimated to be −2.80 eV, −2.87 eV and −2.83 eV respectively. It was found that the HOMO levels of the dyes in this series are sufficiently lower than the iodine/iodide redox potential value and the LUMO levels of these dyes are sufficiently higher than the bottom of the conduction band of TiO_2 (−4.4 eV), indicating that the electron injection process from the excited dye molecule to TiO_2 conduction band is energetically permitted. From these values, we can find that the introduction of rhodanine-3-acetic acid units into molecules elevated the HOMO level, due to the extension of the π-conjugation as mentioned above. They reduced the gap between the HOMO level and the redox potential of iodine/iodide in **F2** which may be one of the reasons that reduces the efficiency of regeneration of the oxidized dye by I^- and the overall solar-to-electrical energy conversion efficiency [16,17]. By changing the spacer (thiophene or phenyl unit) and acceptor moiety (cyanoacrylic or rhodanine-3-acetic acid group), we can attain different HOMO and LUMO levels. This screening strategy helps us to optimize the TiO_2–dye–hole transporting material system in terms of balance between photovoltage, driving forces and spectral response for future preparation of highly efficient dyes by matching suitable donor–spacer–acceptor components [18].

3.4. Quantum chemical calculation

To gain insight into the geometrical and electronic properties of DSSCs based on these fluoranthene dyes, density functional theory (DFT) calculations [19] were performed at a B3LYP/6-31 + G(d) level for the geometry optimization. The optimized ground state geometries of **F1**, **F2** and **F3** are shown in Fig. 4. It can be clearly seen that except the two benzene rings at the 7- and 12- of fluoranthene, the rest of **F3** is in the same plane. As for **F1** and **F2**, the angle formed between the benzene ring and the thiophene group is computed to be 38.6° and 39.1°, respectively. In **F1** the cyanoacrylic acid group was found to be essentially coplanar with respect to the thiophene unit, reflecting the strong conjugation across the thiophene–cyanoacrylate groups. While in **F2** the carboxyl group is almost vertical to the plane formed by the thiophene and rhodanine groups, we suppose that it will have an unfavorable effect on its anchoring onto the TiO_2 film. The isodensity plots of the frontier molecular orbitals of **F1**, **F2** and **F3** are presented in Fig. 5. On the whole, for all the frontier orbitals shown here, there is virtually no electron density distributed on the two benzene rings at the 7- and 12- of fluoranthene and the carboxylic group in **F2**, which are tilted

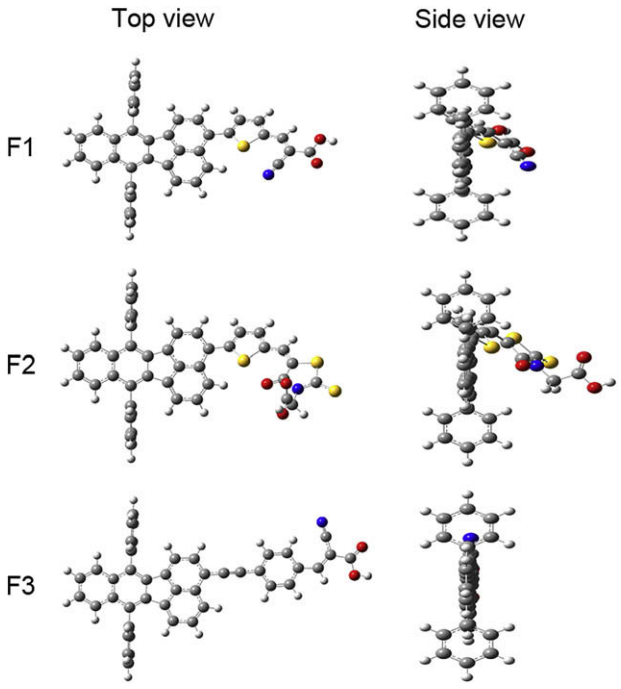

Fig. 4. The optimized ground state structures of **F1**, **F2** and **F3**.

out of the main plane. The HOMO is delocalized over fluoranthene and thiophene/benzene moieties. The LUMO is a π* orbital delocalized across the thiophene/benzene and cyanoacrylic/rhodanine groups; The frontier MOs of (**F1**–**F3**) reveal that HOMO–LUMO excitation moves the electron density distribution from the fluoranthene moiety to the cyanoacrylic acid or rhodanine-3-acetic acid moiety (see Fig. 5).

3.5. Performances of dye-sensitized solar cells

Fig. 6 shows the incident monochromatic photon-to-current conversion efficiency (IPCE) obtained with a sandwich-type two electrode cells. The dye-coated film was used as working electrode,

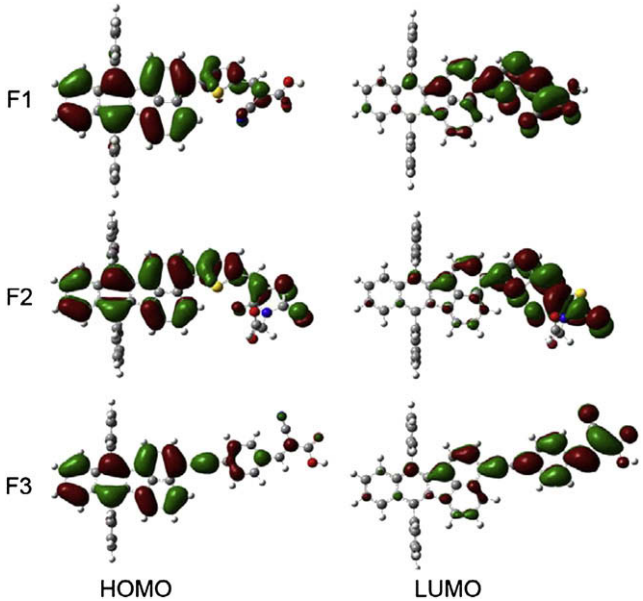

Fig. 5. The frontier orbitals of **F1**, **F2** and **F3** optimized at the B3LYP/6-31G(d) level.

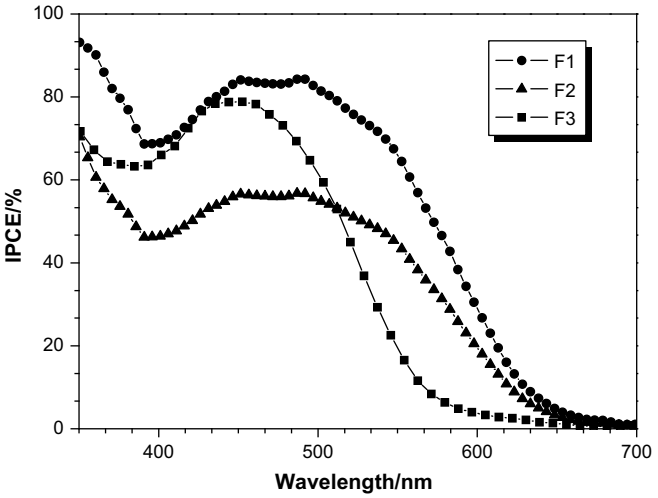

Fig. 6. Photocurrent action spectra of the TiO_2 electrodes sensitized by dyes.

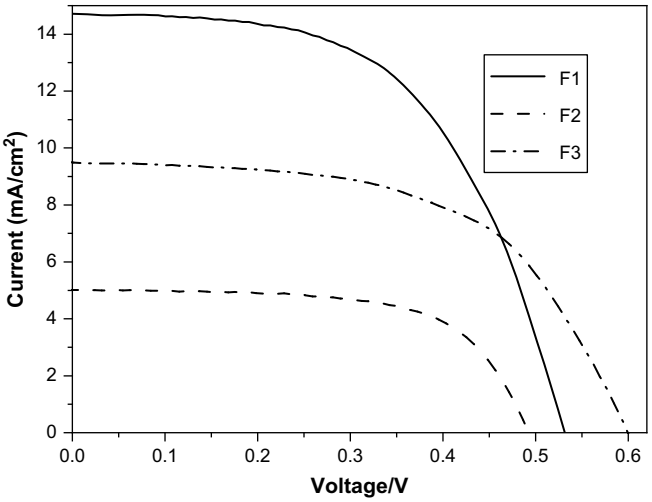

Fig. 7. Photocurrent–voltage curves of dye-sensitized TiO_2 electrodes.

platinized ITO glass as counter electrodes and 0.5 M LiI, 0.05 M I_2 in acetonitrile and 3-methyl-2-oxazolidinone (volume ratio: 9:1) mixture solution as electrolyte. From Fig. 6 one can see that all three dyes can efficiently convert visible light to photocurrent in the region from 400 nm to 700 nm. The IPCE values exceed 68% for **F1** and 46% for **F2** in the spectral range 400–540 nm, respectively, which reaches its maximum of 84% for **F1** at 487 nm and 56% for **F2** at 485 nm. The IPCE performance of the DSSCs with **F1** is higher than that with **F2**, although the action spectra for **F1** are similar to that for **F2** (Fig. 6). It may be one reason that decreases the dye adsorption in TiO_2 (see Table 1) due to steric hindrance of **F2** (Fig. 4). On the other hand, the IPCE efficiencies of **F3** are higher than that of **F2** in the region from 400 nm to 507 nm, though the IPCE values of **F3** than **F2** are lower in the region 510–667 nm (see Fig. 6), suggesting that **F3** sensitized TiO_2 electrode would generate a higher conversion yield compared with **F2**. The rather low IPCE value for **F2** dye indicates that rhodanine-3-acetic acid is a poor anchoring group in comparison to cyanoacrylic acid. We have noted that the IPCE spectrum of **F1** is red-shifted compared with the absorption spectrum of the dye adsorbed on TiO_2 (Fig. 3). It may be that the matching of the electrode surface state with **F1** energy level makes a contribution for electricity. The detailed reason for this needs further studies.

Photovoltaic performances of the **F1**–**F3** sensitized TiO_2 film electrodes under standard global AM 1.5 illumination (100 mW cm^{-2}) are listed in Table 2, and the corresponding photocurrent–voltage curves are shown in Fig. 7. **F1** shows the highest efficiency among the three dyes. The open-circuit photovoltage and overall yield for the three dyes lie in the order **F1** > **F3** > **F2**. The short-circuit current and open-circuit voltage of **F2** are lower than **F1** and **F3**, which can be attributed to the poor injection efficiency of the dyes. This may be the result of the small energy gap between electrolyte and dyes [13]. The larger short-circuit current of **F1** than **F3** can be tentatively attributed to thiophene unit electron transfer from the fluoranthene group to the acceptor moiety. The open-circuit voltage of **F3** is higher than **F1**, for the lower-lying HOMO of **F3** which might be beneficial for retarding the electron transfer from TiO_2 to the oxidized dye or electrolyte, which would enhance the open-circuit voltage [16]. The results are consistent with IPCE values and conversion efficiencies under standard global AM 1.5 illumination.

Table 2
Performance parameters of dye-sensitized solar cells.[a]

Dye	J_{sc} (mA cm^{-2})	V_{oc} (V)	FF	H (%)
F1	14.71	0.53	0.56	4.4
F2	5.02	0.50	0.64	1.6
F3	9.53	0.59	0.66	3.7
N719	15.60	0.69	0.62	7.03

[a] The listed data are results from the measurement which has the closest values to the average of 6 times measurements.

4. Conclusion

In summary, three novel organic sensitizers, in which 7, 12-diphenylbenzo[*k*]fluoranthene moiety is acted as electron donor, phenyl and thiophene units as electron spacers and carboxylic acid as electron acceptor, have been designed and synthesized. They are successfully adsorbed on nanocrystalline anatase TiO_2 particles, and subsequently efficient dye-sensitized solar cell has been fabricated. The absorption spectra, electrochemical and photovoltaic properties of the three dyes were extensively studied. It was found that thiophene moiety and the rhodanine-3-acetic acid extends the π-conjugation system of dyes. Moreover, the HOMO and LUMO energy levels tuning can be conveniently accomplished by changing the spacer and acceptor moiety. We obtained a maximum solar energy to electricity conversion efficiency of 4.4% (J_{sc} = 14.71 mA cm^{-2}, V_{oc} = 0.53 V, *ff* = 0.56) under AM 1.5 solar simulator (100 mW cm^{-2}) based on **F1**. This molecular design opens up the possibility of preparing new dye molecules for DSSCs utilizing fluoranthene as electron donor. Future improvement of the power conversion efficiency in fluoranthene-based TiO_2 cell will be possible by modification of the structure, and these works are now in progress.

Acknowledgement

This work was supported by NSFC/China (20772031), National Basic Research 973 Program (2006CB806200) and Scientific Committee of Shanghai. We are grateful to Dr. Yaoquan Tu and Prof. Hans Ågren in the Department of Theoretical Chemistry at the Royal Institute of Technology in Sweden for computational assistance.

References

[1] O'Regan B, Grätzel M. Nature 1991;353:737.

[2] Hagberg DP, Yum JH, Lee H, Sun LC, Grätzel M. Journal of the American Chemical Society 2008;130:6259;
Kroeze JE, Hirata N, Koops S, Nazeeruddin MK, Schmidt-Mende L, Grätzel M. Journal of the American Chemical Society 2006;128:16376.
[3] Ning ZJ, Zhang Q, Tian H. The Journal of Organic Chemistry 2008;73:379;
Chen ZG, Li FY, Huang CH. Current Organic Chemistry 2007;11:1241.
[4] Hara K, Sayama K, Ohga Y, Shinpo A, Suga S, Arakawa H. Chemical Communications 2001;569;
Wang ZS, Cui Y, Hara K, Dan-Oh Y, Kasada C, Shinpo A. Advanced Materials 2007;19:1138;
Hara K, Kurashige M, Danoh Y, Kasada C, Shinpo A, Suga S, et al. New Journal of Chemistry 2003;27:783.
[5] Horiuchi T, Miura H, Uchida S. Chemical Communications 2003;24:3036;
Horiuchi T, Miura H, Sumioka K, Uchida S. Journal of the American Chemical Society 2004;126:12218.
[6] Kitamura T, Ikeda M, Shigaki K, Inoue T, Anderson NA, Lian T, et al. Chemical Materials 2004;16:1806;
Hara K, Kurashige M, Ito S, Shinpo A, Suga S, Sayama K, et al. Chemical Communications 2003;2:252.
[7] Yao QH, Shan L, Li FY, Yin DD, Huang CH. New Journal of Chemistry 2003;27:1277;
Chen YS, Chao L, Zeng ZH, Wang WB, Wang XS, Zhang BW. Journal of Materials Chemistry 2005;15:1654;
Yao QH, Meng FS, Li FY, Tian H, Huang CH. Journal of Materials Chemistry 2003;13:1048.
[8] Zhan WH, Wu WJ, Hua JL, Jing YH, Meng FS, Tian H. Tetrahedron Letters 2007;48:2461;
Ma XM, Hua JL, Wu WJ, Jing YH, Meng FS, Tian H. Tetrahedron 2008;64:345.
[9] Debad JD, Morris JC, Lynch V, Magnus P, Bard A. Journal of the American Chemical Society 1996;118:2374;
Fabrizio EF, Prieto I, Bard A. Journal of the American Chemical Society 2000;122:4996;
Kertesz M, Ashertehrani A. Macromolecules 1996;29:940.
[10] Kuninobu Y, Nishina Y, Takai K. Tetrahedron 2007;63:8463;
Xu ZC, Qian XH, Cui JN, Zhang R. Tetrahedron 2006;62:10117;
Mitchell RH, Chaudhary M, Williams RV, Fyles R, Gibson J, Ashwood MJ, et al. Canadian Journal of Chemistry – Revue Canadienne de Chimie 1992;70:1015.
[11] Nazeeruddin MK, Kay A, Rodicio I, Humphry-Baker R, Grätzel M. Journal of the American Chemical Society 1993;115:6382.
[12] Debad JD, Morris JC, Magnus P, Bard AJ. Journal of Organic Chemistry 1997;62:530.
[13] Hagberg DP, Marinado T, Karlsson KM, Nonomura K, Peng Q, Boschloo G, et al. Journal of Organic Chemistry 2007;72:9550.
[14] Qin P, Yang XC, Chen RK, Sun LC. Journal of Physical Chemistry C 2007;111:1853;
Kim D, Lee JK, Kang SO, Ko J. Tetrahedron 2007;63:1913.
[15] Guo M, Diao PY, Ren J, Meng FS, Tian H. Solar Energy Materials and Solar Cells 2005;88:23.
[16] Chen RK, Yang XC, Tian HN, Wang XN, Hagfeldt A, Sun LC. Chemistry of Materials 2007;19:4007.
[17] Wang ZS, Li FY, Huang CH, Wang L, Wei M, Jin LP, et al. Journal of Physical Chemistry B 2000;104:9676;
Justin Thomas KR, Hsu YC, Lin JT, Lee KM. Chemistry of Materials 2008;20:1830.
[18] Leriche P, Frère P, Cravino A, Alévêque O, Roncali J. Journal of Organic Chemistry 2007;72:8332.
[19] Qin P, Yang XC, Chen RK, Sun LC, Marinado T, Edvinsson T, et al. The Journal of Physical Chemistry C 2007;111:1853.
[20] Dreuw A, Head-Gordon M. Journal of the American Chemical Society 2004;126:4007.